JBUON 2016; 21(1): 208-220
ISSN: 1107-0625, online ISSN: 2241-6293 • www.jbuon.com
E-mail: editorial_office@jbuon.com

ORIGINAL ARTICLE

Identification of biomarkers and pathway-related modules involved in ovarian cancer based on topological centralities

Deng-kui Zhai[1], Bin Liu[2], Xue-feng Bai[3], Jing-ai Wen[4]

[1]Department of Pharmacy, The First Affiliated Hospital of Harbin Medical University, Harbin 150001, Heilongjiang Province, China; [2]Department of Pharmacy, Harbin Children's Hospital, Harbin 150010, Heilongjiang Province, China; [3]Department of Pharmacy, Mudanjiang City Second People's Hospital, Mudanjiang157013, Heilongjiang Province, China; [4]Department of Pharmacy, Red Flag Hospital, Mudanjiang Medical College, Mudanjiang157011, Heilongjiang Province, China

Summary

Purpose: *The present study was designed to explore the significant biomarkers and pathway-related modules for predicting the effects of eribulin relative to paclitaxel in ovarian cancer.*

Methods: *The gene expression data E-GEOD-50831 were downloaded from the European Bioinformatics Institute (EBI) database. Differentially expressed genes (DEGs) were screened. Subsequently, differential coexpression network was constructed. Kyoto Encyclopedia of Genes and Genomes (KEGG) pathway analysis and pathway-related modules mining were conducted. Topological centralities (degree, betweenness, closeness and stress) analyses for coexpression network and pathway-related modules were performed to explore hub genes and the most significant pathways. Then, we verified our findings in an independent sample set via RT-PCR and Western blotting.*

Results: *Centralities results of ESCO1, CDC27and MCM4 ranked the top five. Moreover, among the top 10% hub genes, CDC27, MCM4 and SOS1 were pathway-enriched genes in two networks. A total of 5 and 6 pathway-related modules were obtained under two drugs treatment. Based analyses of degree, betweenness and other centralities, DNA replication pathway-related module was the most significant under paclitaxel treatment, while cell cycle pathway-related module was the most significant under eribulin treatment. RT-PCR and Western blotting results were consistent with the bioinformatics results. The expression level of MCM4 was remarkably decreased under eribulin treatment relative to paclitaxel.*

Conclusions: *The inhibition of ovarian cancer growth by paclitaxel and eribulin might be connected with downregulation of cell cycle and DNA replication pathway. Moreover, MCM4 signature might be a potential biomarker to predict the effect of eribulin in ovarian cancer.*

Key words: *differential co-expression network, differentially expressed genes, eribulin, ovarian cancer, paclitaxel, topological centrality*

Introduction

Ovarian cancer is the most lethal malignancy in females. Remarkably, there will be 22240 estimated new cases and 14180 estimated deaths from ovarian cancer in 2015 in USA, based on SEER data. Though advanced ovarian cancer patients are treated by platinum-based chemotherapy, the 5-year overall survival is 45% in United States and worse in the developing countries because of the high recurrence rate and the resistance to platinum-based chemotherapy [1,2]. Seeking reliable therapeutic drugs with the ability to eliminate ovarian cancer cells has become a great challenge.

Taxanes were applied as antineoplastic drugs

Correspondence to: Jing-ai Wen, MM. Department of Pharmacy, Red Flag Hospital, Mudanjiang Medical College, Tongxiang Road No. 4, Mudanjiang 157011, Heilongjiang Province, China. Tel and Fax: +86 0453 6582800, E-mail: wenjingai157011@163.com
Received: 15/07/2015; Accepted: 10/08/2015

Table 1. The details of the 21 ovarian cell lines

No	*Cell line*	*No*	*Cell line*	*No*	*Cell line*
1	A2780	8	COV644	15	OVCAR-4
2	CaOv3	9	EFO-21	16	OVISE
3	COLO 720E	10	EFO-27	17	OVSAHO
4	COLO-704	11	KURAMOCHI	18	OVTOKO
5	COV362	12	OV56	19	SK-OV-3
6	COV434	13	OV-90	20	TOV-112D
7	COV504	14	OVCAR-3	21	TOV-21G

because of high activity and relatively less toxicity [3]. Paclitaxel, a member of the taxanes' family, is a microtubule-stabilizing mediator and alters the microtubule dynamics which are essential to maintain cellular structure and important to bring off cellular functions, for example, cell cycle [4,5]. Paclitaxel is used in the first-line treatment of advanced ovarian cancer [6]. However, several gene alterations connected with paclitaxel resistance such as beta-tubulin mutations [7], upregulation of stathmin [8] and p53 mutation [9] have limited its use. Another novel and potential microtubule-targeting modulator is eribulin (previously named E7389), which has shown effectiveness in treating cancer [10]. In the xenograft model of human ovarian cancer using BALB/c nude mice, eribulin administration increased the survival and decreased the tumor size as well as number of metastases [10]. Moreover, the activity of eribulin was superior to that of paclitaxel [10]. Nevertheless, few studies have explored the molecular mechanism for predicting the effects of eribulin relative to paclitaxel.

With the aim of exploring the novel and remarkable pathways for predicting the effects of eribulin compared to paclitaxel, we utilized the microarray expression data of ovarian cancer cell lines to identify the DEGs between paclitaxel- or eribulin-treated group and control group, respectively. Moreover, differential coexpression network construction, Kyoto Encyclopedia of Genes and Genomes (KEGG) pathway enrichment and pathway-related module analysis of DEGs were conducted. Subsequently, topological centralities including degree, closeness, betweenness as well as stress were applied to obtain the most significant pathways. Finally, we verified our findings by means of RT-PCR and Western blot. The purpose of our study was to shed some light in the understanding of mechanisms on how ovarian cancer initiates and progresses. Moreover, candidate genes and pathway-related modules extracted by our method might provide the groundwork for the therapy for ovarian cancer.

Methods

Data acquisition

The gene expression profile numbered E-GEOD-50831 [11] which was based on the GPL570 platform of [HG-U133_Plus_2] Affymetrix Human Genome U133 Plus 2.0 Array was downloaded from EBI database. In this study, gene microarray data contained 189 samples, including 21 ovarian cancer cell lines treated with eribulin, 21 ovarian cancer cell lines treated with paclitaxel and 21 untreated cell lines as control group, all in triplicate. The details of the 21 ovarian cell lines are shown in Table 1.

Data preprocessing and DEGs screening

The gene profile data of E-GEOD-50831 were preprocessed using EXPRESSO function from the Affy package [12]. Background adjustment was carried out using robust multiarray average (RMA) method of Limma package. Subsequently, normalization was performed using the quartile function. Afterwards, microarray suite 5.0 (MAS) was utilized to perform the PerfectMatch (PM) and mismatch match (MM) probe correction. Then, the expression summary was implemented based on MEDIANPOLISH, followed by filtration of the probe data by means of FeatureFilter function. Finally, probe ID was transformed to gene symbol.

To screen key genes in ovarian cancer treated with eribulin and paclitaxel, DEGs were detected using the significant analysis of microarrays (SAM) R package compared with control samples. The Benjamini & Hochberg false discovery rate (FDR) approach [13] was employed to adjust the raw p-value into the false discovery rate (FDR). Genes were regarded to be differentially expressed when FDR<0.05. To increase the stringency for significant difference in gene expression, delta value was defined using the function of SAMR.

compute.delta.table. DEGs in ovarian cancer treated with paclitaxel were selected based on delta cut-off value of 1.188. Moreover, DEGs were ranked in ovarian cancer treated with eribulin when delta value = 1.272.

Construction of differential coexpression network

EBcoexpress package [14] is an empirical Bayesian approach to identify the differential coexpression among gene pairs. In the current study, we used EBcoexpress package to discover the differential coexpression gene pairs in ovarian cancer treated with eribulin and paclitaxel, respectively. Subsequently, Cytoscape (http://cytoscapeweb.cytoscape.org/) [15] was employed to visualize the differential coexpression network.

Topological centralities

To understand the functionality of complex networks of genes, we described the biological importance of genes over indices of topological centrality related to the local scale (degree) and the global scale (betweenness, closeness and stress). Among these, degree is an evident measure of centrality and is defined as the number of links that a node has with its adjacent nodes [16]. Nodes with higher connectivity degrees are named "hubs", suggesting a central role in the network [17]. Betweenness is one of the most popular centrality measures and it ranks the importance of nodes through calculating the shortest paths in the network. Closeness is a measure of the mean length of the shortest paths to access all other proteins in the network [18]. Stress is defined as the number of nodes in the shortest path between two other nodes.

KEGG pathway enrichment analysis and pathway-related module analysis

KEGG (http://www.genome.jp/kegg/) is a bioinformatics resource containing a variety of biochemistry pathways [19]. To fully understand the functions of DEGs between control and treated samples, KEGG pathway analysis of DEGs was implemented using DAVID Bioinformatics Resources 6.7 (http://david.abcc.ncifcrf.gov) [20]. The EASE score was applied to assess the significant categories. Pathways were regarded as having significant difference when $p<0.05$ and gene counts > 2.

Next, we identified pathway-related modules from the differential coexpression network. In an attempt to realize this, we mapped the pathway-related genes to the differential coexpression networks. Subsequently, we extracted the pathway-related modules of these pathway-related genes with the nodes cutoff of 5. Then, topological analyses of degree, betweenness, closeness and stress for the genes of each pathway-related module were carried out. By comparing these topological properties, we obtained the most significant pathway-related modules in cancer treated with paclitaxel and eribulin.

Validation test of effects of eribulin and paclitaxel on key genes

Patients

Overall, 20 primary ovarian cancer patients were included in our study. These 20 cases were treated with drugs as treatment group, while the same patients before treatment made up the control group. Then, we subdivided the treatment group into two subgroups (10 patients receiving paclitaxel and 10 eribulin) according to different drug usage. The mean patient age ranged from 24 to 66 years, and the average age was 35±2.3 years. Importantly, no significant differences in age, sex, case history and region distribution were noticed. All cases were recruited between May 2013 and March 2014 from the Department of Gynecology of our hospital. The experimental protocol was approved by the Human Research Ethics Committee and the Confidentiality of Health Information Committee of our hospital. Tumor tissues in the treated group and ovarian epithelial tissue in the control group were obtained to implement the subsequent experiments.

RT-PCR analysis

Total RNA was isolated from the ovarian cancer cells using RNA extraction kit (Invitrogen, Carlsbad, CA, USA). Then, cDNA was synthesized using the SuperScript II RNase H reverse transcriptase (Invitrogen, Carlsbad, CA, USA). The cDNAs were sub-packaged and stored at -20℃ .

Synthesized cDNA was used as template, and β-actin was applied as an internal control for PCR amplification, respectively. The sequence of primers and length of DNA sequencing are illustrated in Table 2. PCR amplification was performed using the experimental run protocol as follows: 10.0 μl 10×PCR buffer, 1.0 μl TaqDNA polymerase (5 U/μl), 3.0 μl upstream primers, 3.0 μl downstream primers as well as 8.0 μl dNTPs. The amplification conditions are depicted in Table 3. PCR products were electrophoresized on a 1.5% agarose gel at 100 mV for 30 min and analyzed by means of Quantity One software. The experiment was repeated three times and plotted by means of the average value of data.

Western blotting

Total proteins were extracted with 1 mM phenylmethanesulfonyl fluoride (PMSF) in 1 ml ice-cold RIPA buffer (Beyotime, Nanjing, China). Then, these were added to EDTA-free protease inhibitor cocktail. Subsequently, protein concentrations were examined by means of bicinchoninic acid protein assay. Protein extracts (10 μg) were separated by 12% SDS-PAGE, and then transferred onto NC membrane (KENKER, Vancouver, Canada). Afterwards, the NC membranes were blocked with 5% nonfat milk in TBST buffer at 37°C for 2 hrs. Then, the membranes were incubated at 37°C

Table 2. Sequence of primers and length of DNA sequencing

Genes	*Primer sequence (5'-3')*	*Length (bp)*
ESCO1	F: GCTGAATACCCTGATGGCAGGA R: GGAATAGCACATTAGTGGAGCCT	135
CDC27	F: ACACCTCCTGTAATTGATGTGCC R: GGAGTTACCTCTCGGCTATTTCC	140
MCM4	F: CTTGCTTCAGCCTTGGCTCCAA R: GTCGCCACACAGCAAGATGTTG	150
SOS1	F: GGAGATCAACCCTTGAGTGCAG R: TGCTCTACCCAGTGCCGACATA	101
β-actin	F: CTCCATCCTGGCCTCGCTGT R: GCTGTCACCTTCACCGTTCC	268

Table 3. Amplification conditions of PCR

Genes	*Response conditions*
ESCO1	Pre-degeneration at 95℃ for 2 min; Degeneration at 94℃ for 30 s, annealing at 58℃ for 30 s, extension at 72℃ for 30s, 40 cycles; Extension at 72℃ for 10 min.
CDC27	Pre-degeneration at 95℃ for 2 min; Degeneration at 94℃ for 1 min, annealing at 62℃ for 30 s, extension at 68℃ for 1 min, 45 cycles; Extension at 72℃ for 7 min.
MCM4	Pre-degeneration at 95℃ for 5 min; Degeneration at 95℃ for 20 s, annealing at 56℃ for 30 s, extension at 72℃ for 30 s, 40 cycles; Extension at 72℃ for 7 min.
SOS1	Pre-degeneration at 95℃ for 10 min; Degeneration at 95℃ for 15 s, annealing at 60℃ for 30 s, extension at 72℃ for 30 s, 40 cycles; Extension at 72℃ for 7 min.
β-actin	Pre-degeneration at 94℃ for 3 min; Degeneration at 94℃ for 60 s, annealing at 56℃ for 30 s, extension at 72℃ for 60 s, 40 cycles; Extension at 72℃ for 7 min.

for 2 hrs with primary antibodies. GAPDH was used as an internal control. Next, the membranes were washed with TBST 3 times for 5 min at room temperature. After that, the horseradish peroxidase (HRP)-conjugated secondary antibody was added and incubated at 37°C for 2 hrs, followed by washing with TBST. Subsequently, substrates were added to the membranes for 3 min, and exposure was performed in the dark. The experiment was repeated three times. Image J software was used to quantify the protein bands.

Statistics

All statistical analyses were carried out with SPSS19.0 package software. All data are shown as means ± standard deviation (SD). Two-group differences were evaluated by paired t-test and a p value less than 0.05 was considered as statistically significant.

Results

Identification of DEGs

A total of 157 DEGs were identified in ovarian cancer cell lines treated with paclitaxel, including 105 up- and 53 downregulated genes, while a total of 184 DEGs including 98 up- and 86 downregulated genes were screened in ovarian cancer cell lines treated with eribulin.

KEGG pathway enrichment analysis

Based on $p<0.05$ and enriched gene counts >2, DEGs in ovarian cancer treated with paclitaxel and eribulin were enriched in 11 and 10 significant pathways, respectively, as shown in Table 4. Almost all of the enriched pathways in these two drugs treated cancer cells were similar. Importantly, progesterone-mediated oocyte maturation pathway was disturbed only in the paclitaxel group. Collectively, the common top 3 pathways were cell cycle, DNA replication and oocyte meiosis in the paclitaxel-eribulin treated ovarian cancer cells.

Construction of differential coexpression network and topological analysis

Totally, there were 3183 and 3544 differential

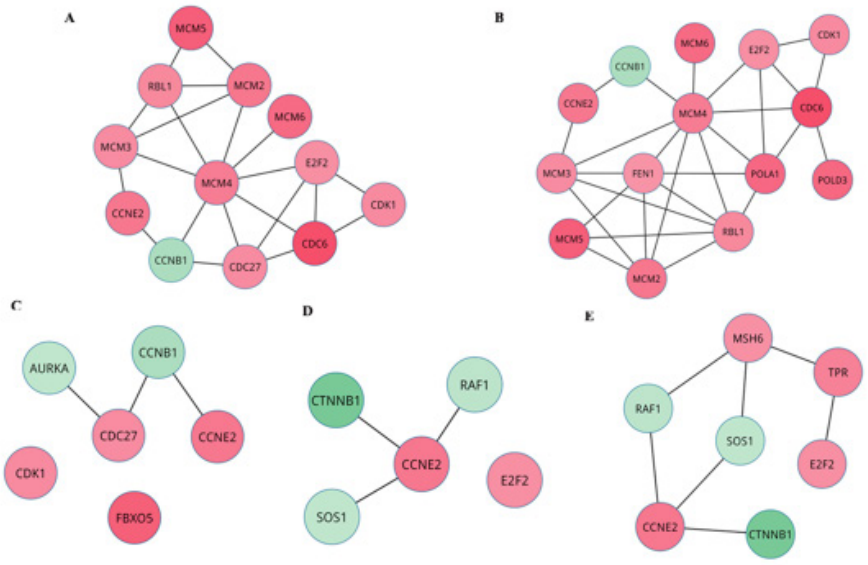

Figure 1. The 5 pathway-related modules of differentially expressed genes (DEGs) in ovarian cancer treated with paclitaxel. The red nodes are the downregulated genes; the green nodes are the upregulated genes. The degrees of color intensity denote fold change value of DEGs. **A**-**E** indicate module 1, module 2, module 3, module 4, and module 5, respectively.

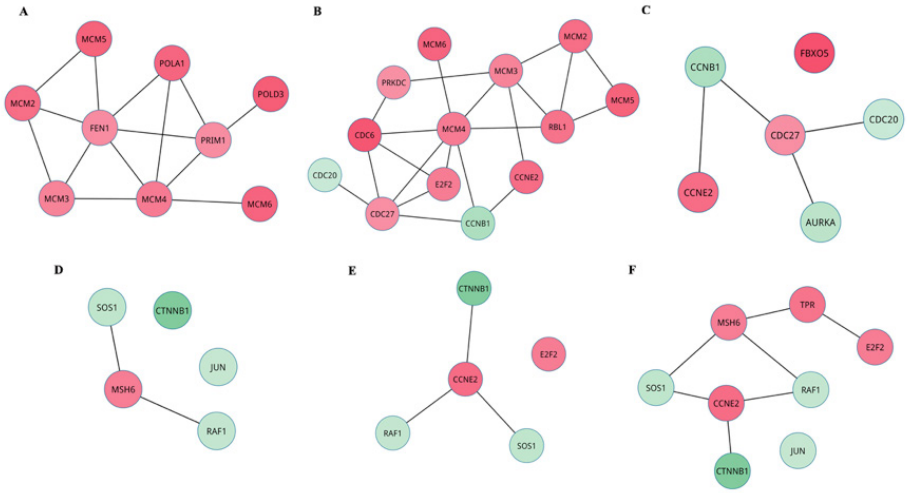

Figure 2. The 6 pathway-related modules of differentially expressed genes (DEGs) in ovarian cancer cells treated with eribulin. The red nodes stand for the downregulated genes; green nodes represent the upregulated genes. The degrees of color intensity denote fold change value of DEGs. **A**-**F** indicate module 1, module 2, module 3, module 4, module 5, and module 6, respectively.

coexpression gene pairs in the coexpression network of ovarian cancer cells treated with paclitaxel and eribulin, respectively.

To further describe the biological importance of nodes, topological centrality analyses of degree, closeness, stress and betweenness for differential coexpression networks were performed. A total of 157 and 185 genes centralities were obtained in the differential coexpression networks of ovarian cancer cells treated with paclitaxel and eribulin, respectively. Moreover, the corresponding topological centralities of the top 10% ranked genes in these two coexpression networks of paclitaxel and eribulin treated cancer are shown in Tables 5

Table 4. Kyoto Encyclopedia of Genes and Genomes (KEGG) enrichment analysis of differentially expressed genes in ovarian cancer treated with paclitaxel and eribulin

Group	*Term name*	*Count*	*p value*
Paclitaxel -treated	Cell cycle	12	2.15E-09
	DNA replication	8	9.11E-09
	Oocyte meiosis	6	0.00174
	Non-homologous end-joining	3	0.00468
	Prostate cancer	5	0.00541
	Mismatch repair	3	0.0144
	Colorectal cancer	4	0.0295
	Progesterone-mediated oocyte maturation	4	0.0314
	Base excision repair	3	0.0319
	Gap junction	4	0.0342
	Pathways in cancer	7	0.0457
Eribulin-treated	DNA replication	9	1.66E-09
	Cell cycle	13	2.57E-09
	Oocyte meiosis	6	0.00500
	Non-homologous end-joining	3	0.00745
	Colorectal cancer	5	0.0103
	Prostate cancer	5	0.0125
	Mismatch repair	3	0.0226
	B cell receptor signaling pathway	4	0.0407
	Pathways in cancer	8	0.0477
	Base excision repair	3	0.0492

and 6, respectively. It was found that the results of various centralities based analyses of the same network were not completely unanimous. Of note, centralities results of *ESCO1* (establishment of sister chromatid cohesion N-acetyltransferase 1) ranked top one in closeness and stress, top two in degree and three in betweenness in the paclitaxel group. In the eribulin group, centralities results of *CDC27* (cell division cycle 27) ranked top one in degree and closeness, and top two in beweenness and stress. Moreover, *MCM4* (minichromosome maintenance complex component 4) ranked top one in betweenness and stress, top two in degree, and top three in closeness. After integrating the results of these 4 centralities, 28 hub genes were extracted in both groups. Among these genes, 4 were pathway-related genes including *CDC27*, *MCM4*, *SOS1* (son of sevenless homolog 1) and *FEN1* (flap structure-specific endonuclease 1). *ESCO1*, *CDC27*, *MCM4* and *SOS1* were extracted for further analysis.

Pathway-related module analysis

After mapping the pathway-related genes to the differential coexpression network, a total of 5 and 6 pathway-related modules were identified in paclitaxel and eribulin groups, respectively (Figures 1 and 2). In the paclitaxel group, we found that module 1-5 matched up with the pathways of cell cycle, DNA replication, oocyte meiosis, prostate cancer, and pathway in cancer, respectively. To further obtain the most significant pathway-related module, we conducted the topological centralities analyses (degree, stress, closeness and betweenness), as shown in Figure 3. Based on the results, module 2 had the highest degree of 497, highest betweenness of 0.0916, highest closeness of 7.85 and highest stress of 31100. Module 1 possessed the second highest topological centralities including degree with 460, betweenness

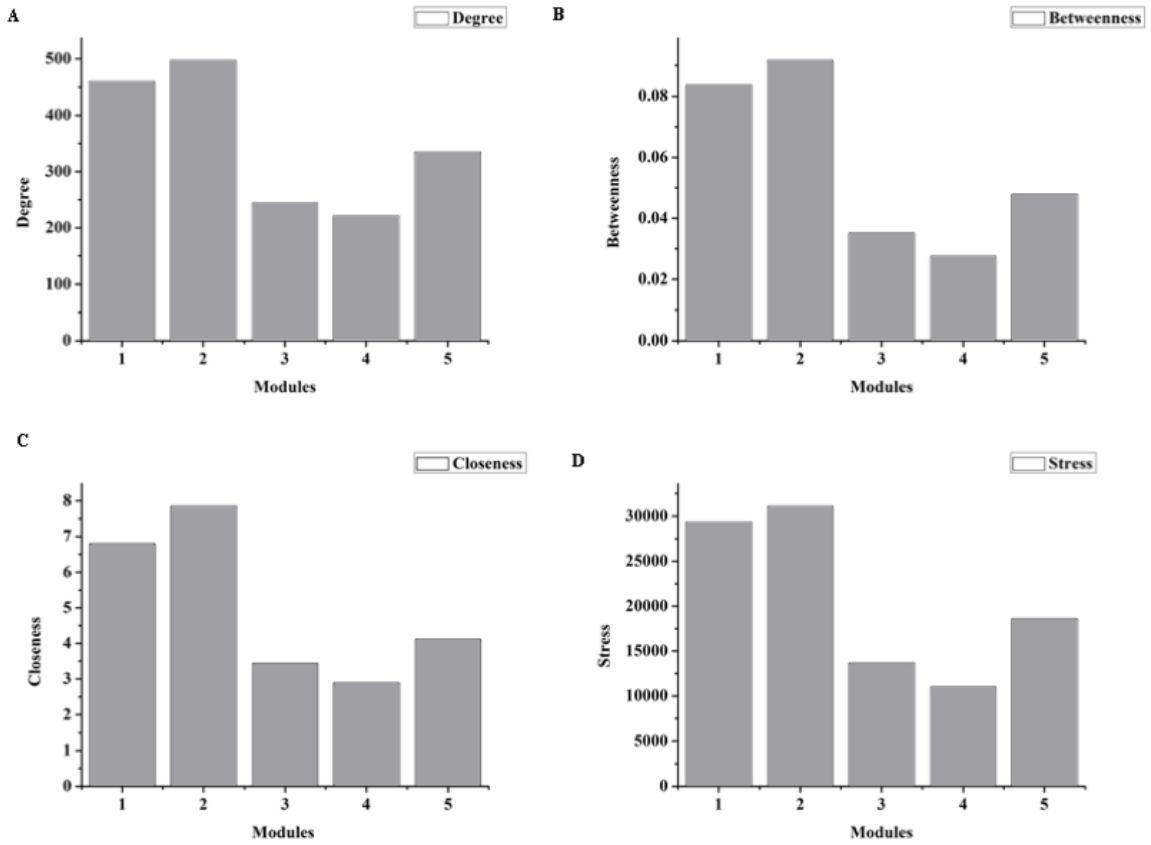

Figure 3. Topological centrality (degree, betweenness, closeness and stress) results of 5 modules in the paclitaxel-treated group.

Table 5. The top 10% ranked genes based on degree, betweenness, closeness and stress in the differential coexpression networks in ovarian cancer treated with paclitaxel

Gene	*Degree*	*Gene*	*Betweenness*	*Gene*	*Closeness*	*Gene*	*Stress*
KRR1	84	MCM4	0.0243	ESCO1	0.684	ESCO1	8366
ESCO1	84	SKIL	0.0221	KRR1	0.681	MCM4	7448
SNRPA1	82	ESCO1	0.0218	SNRPA1	0.675	ZFR	6744
CDC27	82	FEN1	0.0188	CDC27	0.675	SKIL	6610
PPP6R3	81	ARHGEF7	0.0177	PPP6R3	0.672	FEN1	6568
LOC90834	79	MSH6	0.0172	LOC90834	0.670	CDC27	6424
ARHGEF7	78	CDC27	0.0165	MCM4	0.667	ARHGEF7	6202
MCM4	78	PAPOLA	0.0147	ARHGEF7	0.667	MSH6	6140
FEN1	78	TROAP	0.0141	FEN1	0.664	KRR1	5706
SOS1	77	ZFR	0.0138	SKIL	0.664	PPP6R3	5304
MSH6	77	SOS1	0.0137	MSH6	0.664	PAPOLA	5206
SKIL	77	PPP6R3	0.0137	SOS1	0.661	SNRPA1	4984
RNF34	76	MACF1	0.0131	ITFG2	0.658	SOS1	4976
ITFG2	76	KRR1	0.0127	RNF34	0.655	LOC90834	4836
ZFR	75	DEPDC1	0.0124	ZFR	0.655	TROAP	4746
PAPOLA	74	TRAPPC10	0.0124	PAPOLA	0.653	ITFG2	4524

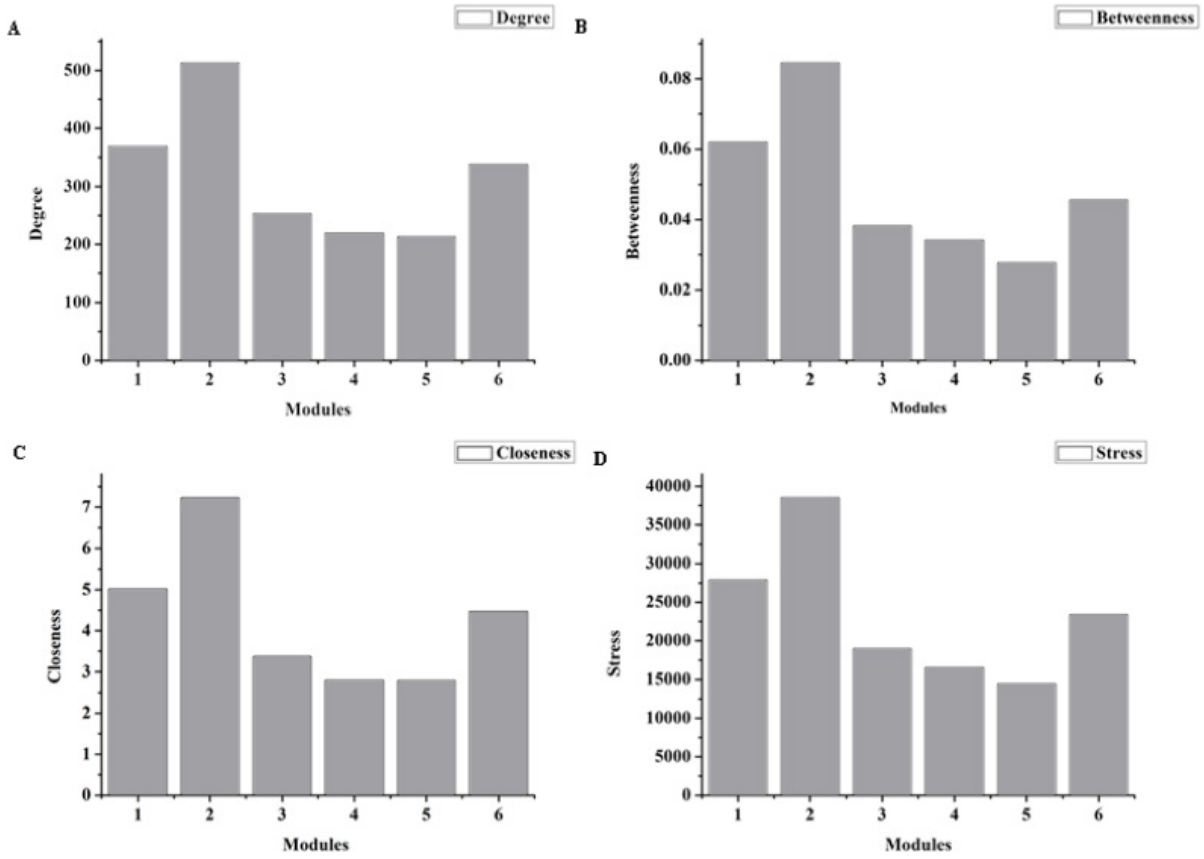

Figure 4. Topological centrality (degree, betweenness, closeness and stress) results of 6 modules in the eribulin-treated group.

with 0.0836, closeness with 6.80 and stress with 29300. Accordingly, DNA replication pathway-related module showed the highest significance. Cell cycle pathway-related module was the second most remarkable one.

Moreover, modules 1-6 matched up with the pathways of DNA replication, cell cycle, oocyte meiosis, colorectal cancer, prostate cancer, and pathway in cancer, respectively. From the topological centralities results (Figure 4), we found that module 2 had the highest topological centralities including degree of 38500, betweenness of 0.0845, closeness of 7.23 and stress of 38500. Module 1 had the second highest topological centralities including degree of 369, betweenness of 0.0619, closeness of 5.02 and stress of 27900. Accordingly, cell cycle pathway-related module was the most significant module. DNA replication pathway-related module was the second most significant one.

Validation test

PCR and Western blotting were used to verify the mRNA and protein expression levels of key genes (*ESCO1*, *CDC27*, *MCM4* and *SOS1*) from bioinformatics analysis. The relative expression level of these genes examined by PCR and western blotting are displayed in Figure 5 and Figure 6, respectively.

We found that the expression of *ESCO1*, *CDC27* and *MCM4* was significantly decreased in ovarian cancer treated with paclitaxel and eribulin relative to control group from RT-PCR and western blotting, which completely agreed with the bioinformatics results. While the expression level of SOS1 was upregulated in paclitaxel and eribulin groups relative to the control group, the differences had no statistical significance except the transcriptional level of SOS1 in the eribulin group. Moreover, no significant difference of *ESCO1*, *SOS1* and *CDC27* was detected between the paclitaxel and eribulin treated groups, while the expression level of *MCM4* was remarkably decreased in eribulin-treated samples relative to that in paclitaxel-treated samples based on the verification results.

Table 6. The top 10% ranked genes based on degree, betweenness, closeness and stress in the differential coexpression network in ovarian cancer treated with eribulin

Gene	*Degree*	*Gene*	*Betweenness*	*Gene*	*Closeness*	*Gene*	*Stress*
CDC27	88	MCM4	0.0238	CDC27	0.658	MCM4	9974
MCM4	87	CDC27	0.0197	LOC90834	0.656	CDC27	9374
LOC90834	87	ESCO1	0.0180	MCM4	0.654	ESCO1	8988
MSH6	82	LOC90834	0.0164	MSH6	0.642	LOC90834	8394
ESCO1	81	KCTD10	0.0161	ESCO1	0.640	NOMO3	7816
KCTD10	77	MSH6	0.0158	KCTD10	0.631	ZFR	7604
FEN1	76	SOS1	0.0149	FEN1	0.629	MSH6	7470
PAPOLA	75	NOMO3	0.0148	PAPOLA	0.629	FEN1	7422
ITFG2	75	DEPDC1	0.0146	ZFR	0.629	KCTD10	7306
ZFR	75	FEN1	0.0145	ITFG2	0.625	SCYL2	7046
SOS1	73	PAPOLA	0.0140	SOS1	0.620	SOS1	6960
AP2A1	72	SCYL2	0.0139	AP2A1	0.618	PAPOLA	6626
DHX9	69	ITFG2	0.0122	DHX9	0.616	DHX9	5958
SUPT16H	69	HECTD1	0.0121	SUPT16H	0.616	DEPDC1	5890
NOMO3	68	MACF1	0.0121	NOMO3	0.612	ITFG2	5824
HECTD1	66	ZFR	0.0101	HECTD1	0.608	HECTD1	5792
7-MAR	65	SFXN3	0.0093	7-MAR	0.606	SUPT16H	5608
CCNE2	65	MAP4K5	0.0092	SCYL2	0.604	SFXN3	5474

Discussion

In the current study, the novel biomarkers and pathway-related modules for predicting the effects of eribulin relative to paclitaxel were analyzed by evaluating topological centralities (degree, betweenness, closeness and stress) for differential co-expression networks and pathway-related modules. Centralities results of *ESCO1*, *CDC27* and *MCM4* ranked the top five. Moreover, *CDC27*, *MCM4*, *SOS1* were pathway-enriched genes in two networks. More importantly, a total of 5 and 6 pathway-related modules were obtained in paclitaxel and eribulin treatments, respectively. Among the extracted modules in the paclitaxel and eribulin groups, cell cycle and DNA replication pathway-related module was the most significant modules. Among the hub genes, *ESCO1*, *CDC27*, *MCM4* and *SOS1* were extracted based on analysis of topological centralities, and the expression verification by RT-PCR and Western blotting was basically consistent with the bioinformatics results.

In the current study, the centrality analyses of pathway-related modules showed that cell cycle and DNA replication pathway-related module was the most significant in the two treatments. Cell cycle is a series of coordinated procedures, which functions to integrate the environment signal pathways with cell proliferation and cell growth [21]. As we know, dysregulation of cell-cycle regulatory mechanisms is a feature of many human cancers including ovarian malignancy [22]. A large number of strategies has been suggested to disturb the cancer cell proliferation through suppressing cell cycle events [23]. Fortunately, paclitaxel and eribulin are a kind of tubulin-targeting agents with the ability to bind to microtubules, to further disturb the formation of mitotic spindle, and finally to induce the cell cycle arrest, resulting in cell death [5,24]. Previously, the alteration of cell cycle pathway after paclitaxel and eribulin treatment has been demonstrated in ovarian cancer [25,26]. Accordingly, cell cycle pathway correlates with the activity of paclitaxel and eribulin in ovarian cancer.

ESCO1, a cohesion-associated gene, is crucially important in the process of sister chromatid cohesion [27]. It is noteworthy that the sister chroma-

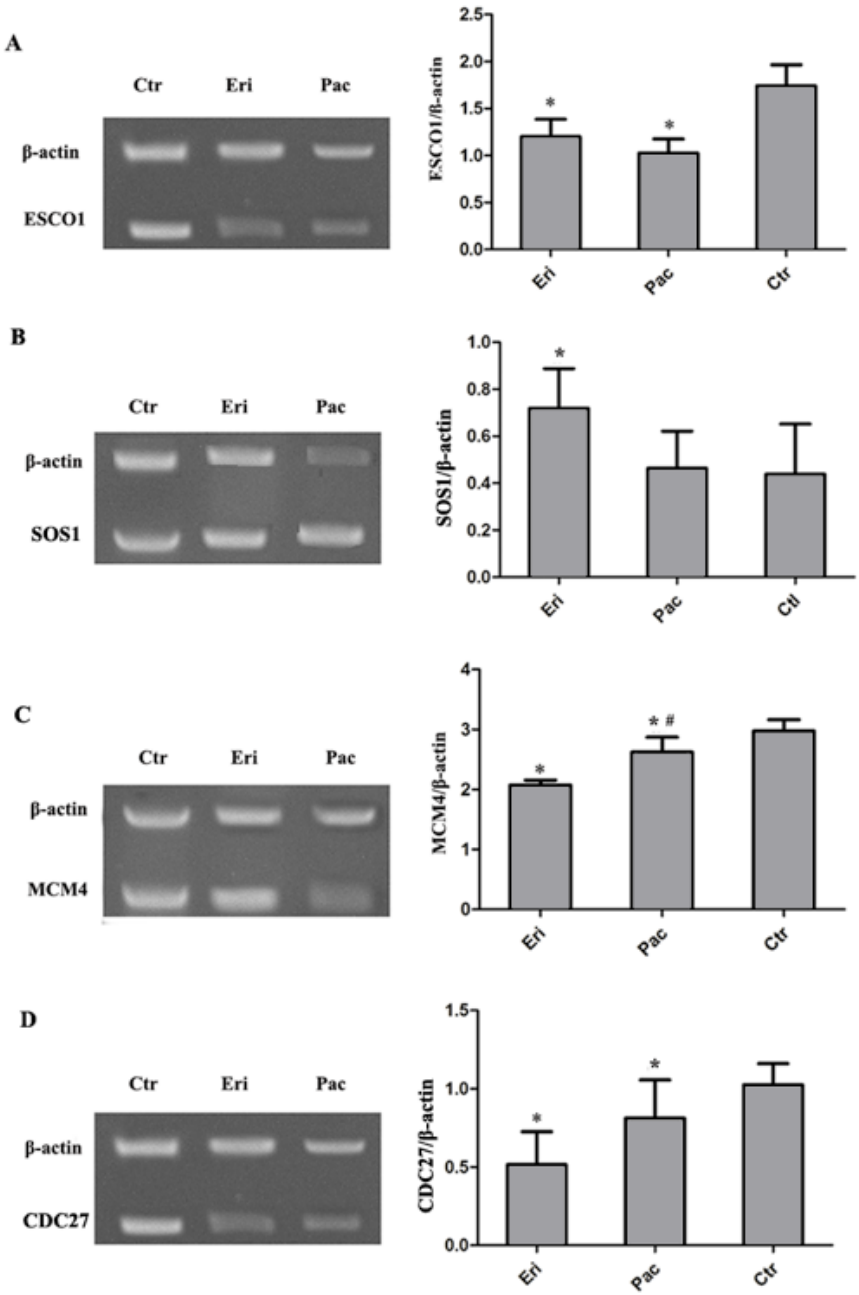

Figure 5. The expression of *ESCO1* (**A**), SOS1 (**B**), MCM4 (**C**) and CDC27 (**D**) as detected by PCR. Eri stands for the samples treated with eribulin, Pac for the samples treated with paclitaxel, Ctr for the control samples. *p<0.05 vs control group; # p<0.05 vs eribulin samples.

tid cohesion plays a pivotal role during the period of DNA replicati on [28]. Furthermore, *ESCO1* was reported to be overexpressed in prostate cancer [29]. *ESCO1* can hamper chromosomal breakage during S phase [30], and the *ESCO1* protein disruption hinders cohesion during G2-M phase in yeast [31]. *MCM4*, a member of minichromosome maintenance protein family, plays a pivotal role in the initiation of DNA replication [32]. Moreover, MCM2-7 proteins gather in the nucleus in G1 phase as well as establish the S phase checkpoint [33]. Previous studies have indicated that increased expression of *MCM4* is detected in many cancers including esophageal cancer as well as cervical squamous cell carcinomas [34,35]. In the present study, *ESCO1* and *MCM4* were downregulated in ovarian cancer treated with paclitaxel and eribulin. Therefore, as demonstrated here, the suppression of paclitaxel and eribulin on the development of ovarian cancer by downregulating *ESCO1* and *MCM4* highlights the underlying application of paclitaxel and eribulin via inducing

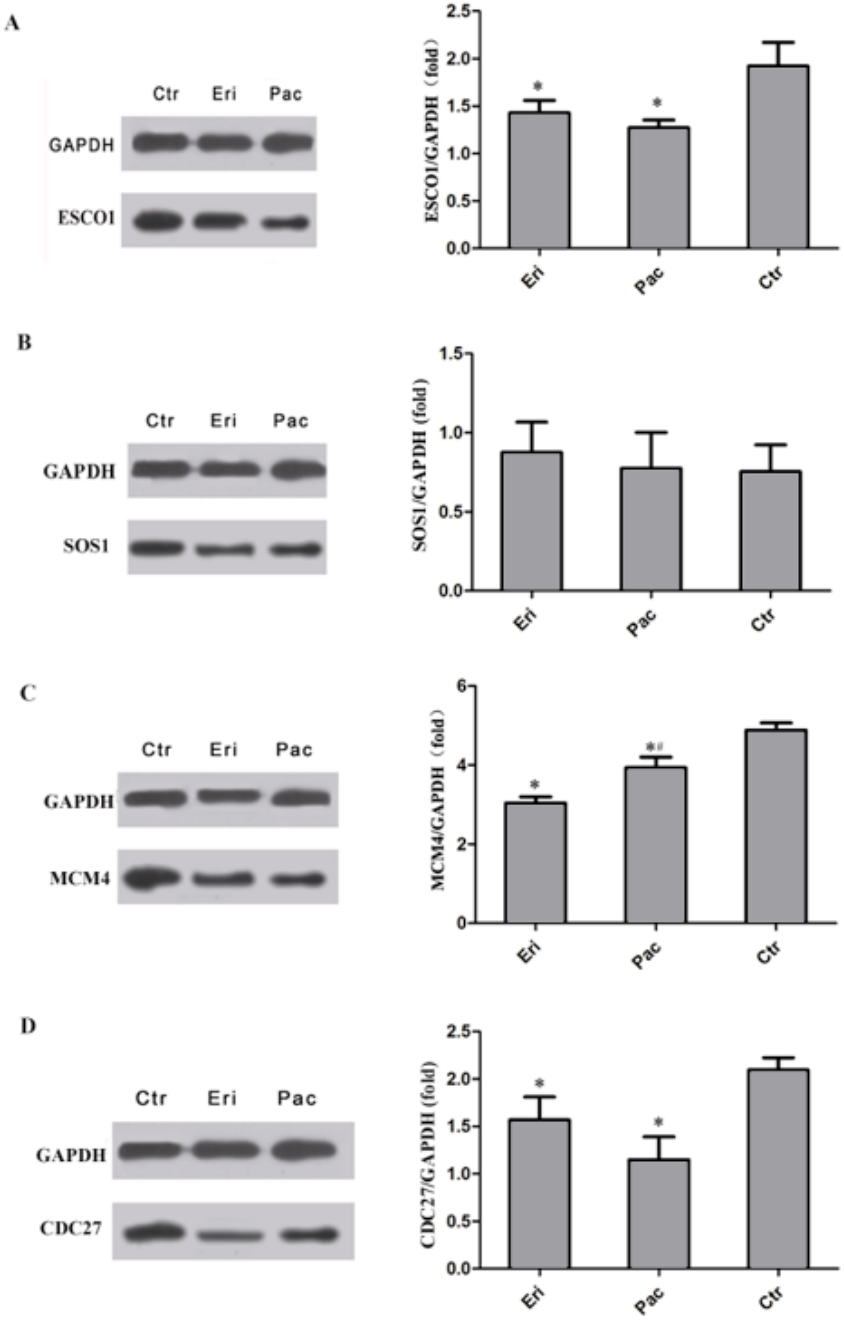

Figure 6. The expression of *ESCO1* (**A**), SOS1 (**B**), MCM4 (**C**) and CDC27 (**D**) as detected by Western blotting. Eri stands for the samples treated with eribulin, Pac for the samples treated with paclitaxel, Ctr for the control samples. * $p<0.05$ vs control group; # $p < 0.05$ vs eribulin samples.

cell cycle arrest in ovarian cancer.

According to PCR and western blotting results, we found no significant difference of *ESCO1* in ovarian cancer treated with paclitaxel and eribulin. The expression level of *MCM4* was remarkably decreased in eribulin-treated samples relative to paclitaxel-treated samples, which suggested that patients with ovarian cancer might benefit more from eribulin administration compared with paclitaxcel administration on the basis of *MCM4* expression. Accordingly, *MCM4* signature might be a potential biomarker to predict the effect of eribulin on ovarian cancer.

Although there remain shortcomings in our study, for example, small sample size, our findings provide proofs that the growth inhibition of ovarian cancer by paclitaxel and eribulin might be related to downregulation of cell cycle and DNA

replication pathway. Moreover, our results suggest that *MCM4* signature might be a potential biomarker to predict the effect of eribulin in ovarian cancer.

References

1. Gapstur S, Jacobs E, Deka A. Association of alcohol intake with pancreatic cancer mortality in never smokers. World Cancer Report 2014. World Health Organization 2014:444-451.
2. Ozols RF, Bundy BN, Greer BE et al. Phase III trial of carboplatin and paclitaxel compared with cisplatin and paclitaxel in patients with optimally resected stage III ovarian cancer: a Gynecologic Oncology Group study. J Clin Oncol 2003;21:3194-200.
3. Crown JP. The platinum agents: a role in breast cancer treatment? Semin Oncol 2001; 28:28-37.
4. Sève P, Dumontet C. Is class III β-tubulin a predictive factor in patients receiving tubulin-binding agents? Lancet Oncol 2008;9:168-175.
5. Perez EA. Microtubule inhibitors: Differentiating tubulin-inhibiting agents based on mechanisms of action, clinical activity, and resistance. Mol Cancer Ther 2009;8:2086-2095.
6. Omura GA. Progress in gynecologic cancer research: the Gynecologic Oncology Group experience. Semin Oncol 2008;35:507-521.
7. Hari M, Loganzo F, Annable T et al. Paclitaxel-resistant cells have a mutation in the paclitaxel-binding region of β-tubulin (Asp26Glu) and less stable microtubules. Mol Cancer Ther 2006;5:270-278.
8. Alli E, Bash-Babula J, Yang J-M, Hait WN. Effect of stathmin on the sensitivity to antimicrotubule drugs in human breast cancer. Cancer Res 2002;62:6864-6869.
9. Wahl AF, Donaldson KL, Faircnild C et al. Loss of normal p53 function confers sensitization to Taxol by increasing G2/M arrest and apoptosis. Nat Med 1996;2:72-79.
10. Towle MJ, Salvato KA, Budrow J et al. In vitro and in vivo anticancer activities of synthetic macrocyclic ketone analogues of halichondrin B. Cancer Res 2001;61:1013-1021.
11. Dezső Z, Oestreicher J, Weaver A et al. Gene Expression Profiling Reveals Epithelial Mesenchymal Transition (EMT) Genes Can Selectively Differentiate Eribulin Sensitive Breast Cancer Cells. PloS One 2014;9:e106131.
12. Gautier L, Cope L, Bolstad BM, Irizarry RA. Affy analysis of Affymetrix GeneChip data at the probe level. Bioinformatics 2004;20:307-315.
13. Benjamini Y, Drai D, Elmer G, Kafkafi N, Golani I. Controlling the false discovery rate in behavior genetics research. Behav Brain Res 2001;125:279-284.
14. Dawson JA, Ye S, Kendziorski C. R/EBcoexpress: an empirical Bayesian framework for discovering differential co-expression. Bioinformatics 2012;28:1939-1940.
15. Smoot ME, Ono K, Ruscheinski J, Wang P-L, Ideker T. Cytoscape 2.8: new features for data integration and network visualization. Bioinformatics 2011;27:431-432.
16. Otte E, Rousseau R. Social network analysis: a powerful strategy, also for the information sciences. J Inf Sci 2002;28:441-453.
17. He X, Zhang J. Why do hubs tend to be essential in protein networks ? PLoS Genet 2006;2:p88.
18. Wasserman S, Faust K. Social Network Analysis: Methods and applications. In: Granovetter M (Ed): Structural analysis in the social sciences. New York, NY, Cambridge University Press, 1994, Series 8.
19. Kanehisa M, Goto S. KEGG: Kyoto encyclopedia of genes and genomes. Nucleic Acids Res 2000;28:27-30.
20. Huang DW, Sherman BT, Lempicki RA. Systematic and integrative analysis of large gene lists using DAVID bioinformatics resources. Nat Protoc 2008;4:44-57.
21. Schwartz GK, Shah MA. Targeting the cell cycle: a new approach to cancer therapy. J Clin Oncol 2005;23:9408-9421.
22. Milde-Langosch K, Riethdorf S. Role of cell-cycle regulatory proteins in gynecological cancer. J Cell Physiol 2003;196:224-244.
23. Manchado E, Guillamot M, Malumbres M. Killing cells by targeting mitosis. Cell Death Differ 2012;19:369-377.
24. Wozniak KM, Nomoto K, Lapidus RG et al. Comparison of neuropathy-inducing effects of eribulin mesylate, paclitaxel, and ixabepilone in mice. Cancer Res 2011;71:3952-3962.
25. Bani MR, Nicoletti MI, Alkharouf NW et al. Gene expression correlating with response to paclitaxel in ovarian carcinoma xenografts. Mol Cancer Ther 2004;3:111-121.
26. L'Espérance S, Bachvarova M, Tetu B, Mes-Masson AM, Bachvarov D. Global gene expression analysis of early response to chemotherapy treatment in ovarian cancer spheroids. BMC Genomics 2008;9:99.
27. Mannini L, Musio A. The dark side of cohesin: the carcinogenic point of view. Mut Res 2011;728:81-87.
28. Atienza JM, Roth RB, Rosette C et al. Suppression of RAD21 gene expression decreases cell growth and enhances cytotoxicity of etoposide and bleomycin in hu-

man breast cancer cells. Mol Cancer Ther 2005;4:361-368.

29. Luedeke M, Linnert CM, Hofer MD et al. Predisposition for TMPRSS2-ERG fusion in prostate cancer by variants in DNA repair genes. Cancer Epidemiol Biomarkers Prev 2009;18:3030-3035.
30. Zhang J, Shi X, Li Y et al. Acetylation of Smc3 by Eco1 is required for S phase sister chromatid cohesion in both human and yeast. Mol Cell 2008;31:143-151.
31. Ünal E, Heidinger-Pauli JM, Koshland D. DNA double-strand breaks trigger genome-wide sister-chromatid cohesion through Eco1 (Ctf7). Science 2007;317:245-248.
32. Labib K, Kearsey SE, Diffley JF. MCM2-7 proteins are essential components of prereplicative complexes that accumulate cooperatively in the nucleus during G1-phase and are required to establish, but not maintain, the S-phase checkpoint. Mol Biol Cell 2001;12:3658-3667.
33. Forsburg SL. Eukaryotic MCM proteins: beyond replication initiation. Microbiol Mol Biol Rev 2004;68:109-131.
34. Huang XP, Rong TH, Wu QL et al. MCM4 expression in esophageal cancer from southern China and its clinical significance. J Cancer Res Clin Oncol 2005;131:677-682.
35. Gan N, Du Y, Zhang W, Zhou J. Increase of Mcm3 and Mcm4 expression in cervical squamous cell carcinomas. Eur J Gynaecol Oncol 2010;31:291-294.